

Modeling of Dissolved Oxygen Profile in a Slurry Reactor

Mohammad F. Abid
Chemical Engineering
Department, University of
Technology, Baghdad-Iraq

Atheel K. Jabir
Chemical Engineering
Department, University of
Nahrain, Baghdad-Iraq.

Saad A. Faiq
Chemical Engineering
Department, University of
Technology, Baghdad-Iraq

Abstract

A mathematical model for a slurry bioreactor was proposed to describe oxygen utilization rate and concentration profiles along the reactor for reactants and products in the bubbly flow regime. The model consisted of transient differential equations representing mass transfer and kinetics of oxygen, biomass and substrates in the liquid phase. The model was validated by comparing with experimental work of other authors and a good agreement was obtained, the absolute average error between model and experimental results was 4.3%. The effects of various operating parameters on the concentration profile of oxygen and biomass were investigated theoretically. The dissolved oxygen concentration was significantly affected by the superficial liquid velocity than that by superficial gas velocity. Unsteady state concentration profile of oxygen showed different behaviors gas and liquid.

Keywords: Modeling, Bioreactor, Slurry (three phase) reactor, growth rate.

1. Introduction

Mathematical models have an important role to play in the optimization of three -phase bioreactor^[1]. Bioreactor models aim to describe the overall performance of the bioreactor and consist of two submodels; a balance/transport sub model that describes mass and heat transfer within and between the various phases of the bioreactor and a kinetic submodel that describes how the growth rate of the microorganism depends on the key local environmental variables. One of two approaches may be taken to describing the growth kinetics. Simple empirical equations may be used or mechanistic models that attempt to describe intraparticle diffusion process related to growth may be proposed^[2]. The majority of current bioreactor models have simple empirical kinetic sub models, since the heterogeneity within many bioreactors means that the balance/transport sub model is already quite complex^[1,2]. For example significant gradients can be expected within bed bioreactor with respect to temperature, moisture and the gas phase O₂

concentration^[3,4]. The balance equations in the dynamic models of such systems are partial differential equations, which require much more computational power to solve than the ordinary differential equations that describe the balances over well-mixed bioreactor. Gas - solid fluidized bed bioreactor provides good mixing and heat removal at the macro scale, greatly simplifying the balance equations, and allowing the assumption that all substrate particles are subjected to identical external conditions^[2].

It is usually of interest to model how the growth of the microorganism causes changes in its environment, because, in turn, the growth of the microorganism depends on the conditions in its local environment. Growth of the microorganism is associated with the consumptions of O₂ and nutrients and production wastes metabolic heat, water, carbon dioxide and various products.

The identity of the components that are incorporated into the model depends on what the model proposes to describe. In some cases only a kinetic equation and an energy balance are written. It has often been assumed that heat production is directly proportional to growth^[5,6,7,8,9], although that is probably not true. In any case the inclusion of maintenance heat production is simple matter^[10].

Even though typically attempts are not made within bioreactor models to predict intraparticle concentration profiles of nutrients and the dependence of growth on local nutrient concentrations, due to the complexity that this would introduce, overall consumption of the solid substrate may be of interest in order to predict gross changes in the substrate bed such as bed shrinkage.

Some models take this dry weight loss into account^[10,11]. Other models have ignored the decrease in total solids weight despite the fact that such decreases occur in reality^[6,7,9].

This could be shortcoming since bed shrinkage can potentially have important effects on bioreactor performance, such as promoting channeling in packed-beds^[12]. Early models describing the overculture of

microorganisms on solid substrate were those of Georgion and Shuler ^[13], which described growth at the surface of a flat slab of substrate with glucose as the substrate, and Mitchell et al. ^[14], which described a similar system but with the use of starch as a substrate, in which case it was necessary to describe the release of glucoamylase by the microorganisms at the surface, the diffusion of the glucoamylase, into the substrate, the hydrolysis of starch by the glucoamylase, the diffusion of the released glucose to the surface and the uptake of glucose at the surface by the microbial biomass. Rajagopalan and Modak ^[15] developed a model that took O₂ diffusion into account and gave a structure to the microbial biomass, treating it as a wet biofilm of constant density. The model described the various steps. Diffusion of glucoamylase within the substrate particle was described as:

$$\frac{\partial C_E}{\partial t} = \frac{D_E}{r^2} \frac{\partial}{\partial r} \left(r^2 \frac{\partial C_E}{\partial r} \right) \quad 1$$

Where **r** is the radial position in the particle, **C_E** is the concentration of the enzyme within the substrate particle, **D_E** is the effective diffusivity of the enzyme within the substrate and **t** is time. It was assumed that the enzyme was liberated into the substrate at the biofilm/particle boundary and could not cross this boundary into the biofilm; also there is no reason to suppose this would be the case in reality. Hydrolysis of starch with the substrate particle was assumed to follow Michaelis-Menten kinetics ^[16]:

$$\frac{\partial C_s}{\partial t} = -K_{cat} C_E \left(\frac{C_s}{K_s + C_s} \right) \quad 2$$

Where **C_s** is the starch concentration within the substrate, **K_{cat}** the catalytic constant of the enzyme and **K_s** the Michaelis-Menten constant for starch. Similarly, models of O₂ reaction and diffusion in biofilms have been used in combination with experimental data for overall O₂ consumption rates to show that in some cases aerial hyphase do not contribute significantly to overall O₂ uptake ^[17] whereas in others they do ^[18]. A more sophisticated model was developed by Rajagopalan et al. ^[19], extending the model of Rajagopalan and Modak ^[5] that described the intraparticle diffusion of glucose and O₂. As with the model of Nandakumar et al. ^[20] there is a sharp biomass/particle interface, but the reaction is not limited to this interface because

of the liberation of enzyme into the substrate and diffusion of the glucose into the biofilm. They arrived at the equation:

$$t = \left[\frac{e_b L^2}{2bD_e C_A} \right] \left(1 + \frac{l_c^2}{L^2} - 2\frac{l_c}{L} \right) \quad 3$$

Where **b** is the stoichiometric coefficient, **e_b** is the molar density of the substrate, **L** is the overall particle size, which remains constant, **D_e** is the effective diffusivity of O₂ in the microbial biomass layer, **C_A** is the O₂ concentration at the outer surface of the microbial biomass layer and **l_c** is the length of the undegraded core of residual substrate. In this paper, the mathematical model for a three-phase fluidized bed bioreactor in wastewater treatment process is proposed to describe the oxygen concentration distribution. The validation of the model is done in comparison with the experimental data extracted from literature and various parameters affecting the performance of the bioreactor are estimated using the model.

2. Principle Assumption

The mathematical model was formulated under the following assumptions:

- (a) Solid particle were considered very small.
- (b) Uniform cross section for the reactor (cylinder).
- (c) Uniform temperature inside the reactor (isothermal).
- (d) Pseudo-two-phase model (slurry + gas).
- (e) Uniform density for the liquid phase.
- (f) Gas hold-up was supposed to be constant.
- (g) No gradient in concentration of radial direction in the gas and slurry phase.

3. Oxygen Transfer and Kinetics Model

Oxygen transfer and uptake in the bioreactor can be described by the following steps:

Transport of oxygen from the bulk gas to the bubble interface

- (1) Transport of oxygen from the bubble interface to the slurry phase where reaction occurs.

- (2) The oxygen uptake rate can be described by the Monod kinetics ^[20].

- (3)

$$r_{O_2} = \frac{\mu_m}{Y_{O_2} (K_{O_2} + C)} \rho \quad ds \quad 4$$

Where μ_m is the maximum specific growth rate (s^{-1}); K_{O_2} is saturation constant of oxygen (gcm^{-3}); ρ_{ds} is the substrate dry density (gcm^{-3}); C is the oxygen concentration dissolved in liquid (gcm^{-3}); Y_{O_2} is yield of biomass upon oxygen. If $C \gg K_{O_2}$, the reaction rate follows the intrinsic zero order kinetics.

$$(-r_{O_2}) = \frac{\mu_m}{Y_{O_2}} \rho_{ds} = K_0 \rho_{ds} \quad 5$$

Where K_0 is the intrinsic zero-order rate constant.

4. Governing Equations of Mathematical Model

Assumptions (f) and (g) characterize a homogeneous flow regime through the reactor. Figure (1) shows a mathematical representation of the bioreactor. Equations of mathematical model were resulted from differential balance along the reactor

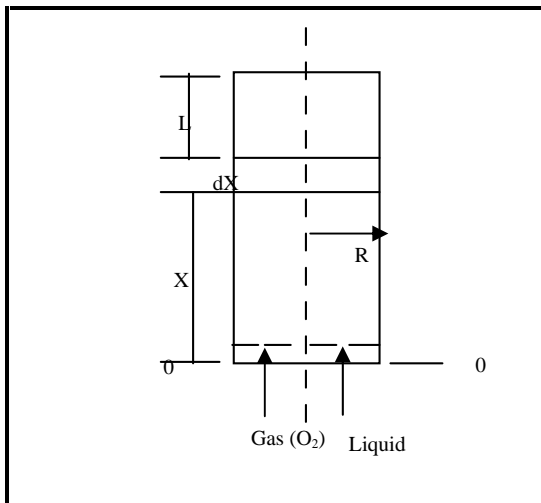


Fig. (1): A mathematical representation of the bioreactor.

$$\frac{\partial C_g}{\partial t} + U_g \frac{\partial C_g}{\partial x} - D_g \frac{\partial^2 C_g}{\partial x^2} = -\frac{K_{LA}}{\varepsilon_g} \left[\frac{C_g}{H} - C_L \right] \quad 6$$

* For oxygen balance in the liquid phase:

$$\frac{\partial C_L}{\partial t} + U_L \frac{\partial C_L}{\partial x} - D_L \frac{\partial^2 C_L}{\partial x^2} = -\frac{K_{LA}}{\varepsilon_L} \left[\frac{C_g}{H} - C_L \right] - \frac{1}{Y_{O_2} M_{O_2}} r_{B1} \quad 7$$

* For biomass balance in the liquid phase:

$$\frac{\partial B_1}{\partial t} + U_L \frac{\partial B_1}{\partial x} - D_L \frac{\partial^2 B_1}{\partial x^2} = r_{B1} \quad 8$$

* For substrate balance in the liquid phase:

$$\frac{\partial C_{SL}}{\partial t} + U_L \frac{\partial C_{SL}}{\partial x} - D_L \frac{\partial^2 C_{SL}}{\partial x^2} = \frac{1}{Y_s} r_{S,1} \quad 9$$

5. Boundary Conditions:

To solve equations (6), (7), (8) and (9) the following boundary conditions are applied:

* For oxygen in the gas phase:

$$\left. \begin{array}{l} \text{at } X=0 \quad C_g = C_{g0} \\ \text{at } X=L \quad \frac{\partial C_g}{\partial X} = 0 \end{array} \right\} \quad 10$$

* For oxygen in the liquid phase:

$$\left. \begin{array}{l} \text{at } X=0 \quad C_L = C_{L0} \\ \text{at } X=L \quad \frac{\partial C_L}{\partial X} = 0 \end{array} \right\} \quad 11$$

* For biomass in the liquid phase:

$$\left. \begin{array}{l} \text{at } X=0 \quad C_{BL} = C_{B0} \\ \text{at } X=L \quad \frac{\partial C_{BL}}{\partial X} = 0 \end{array} \right\} \quad 12$$

* For substrate in the liquid phase:

$$\left. \begin{array}{l} \text{at } X=0 \quad C_{SL} = C_{SL0} \\ \text{at } X=L \quad \frac{\partial C_S}{\partial X} = 0 \end{array} \right\} \quad 13$$

6. Model Solution

The partial differential equation of the model (i.e, eqns. 6 to 9) were approximated into linear algebraic equations by finite difference method [22] and solved numerically by means of MATLAB R2010b for (Computer type).

Let the increment in X and t is h_x and Δt respectively. The following partial differential equation (i.e., equation 8):

$$\frac{\partial C_{Bl}}{\partial t} + U_l \frac{\partial C_{Bl}}{\partial x} - D_L \frac{\partial^2 C_{Bl}}{\partial x^2} = r_{Bl} \quad 14$$

is approximated using the following finite difference formula for first and second derivatives:

$$\frac{\partial C_{Bl}}{\partial t} = \frac{1}{K} [C_{Bl}(t+k, x) - C_{Bl}(t, x)] \quad 15$$

$$\frac{\partial C_{Bl}}{\partial X} = \frac{1}{h_x} [C_{Bl}(t, x+h_x) - C_{Bl}(t, x)] \quad 16$$

$$\frac{\partial^2 C_{Bl}}{\partial X^2} = \frac{1}{h_x^2} [C_{Bl}(t, x+h_x) - 2C_{Bl}(t, x) + C_{Bl}(t, x-h_x)] \quad 17$$

Substitute eqns. (15), (16) and (17) into (14):

$$\frac{1}{K} [C_{Bl}(t+k, x) - C_{Bl}(t, x)] - \frac{U_l}{h_x} [C_{Bl}(t, x+h_x) - C_{Bl}(t, x)] - \frac{D_L}{h_x^2} [C_{Bl}(t, x+h_x) - 2C_{Bl}(t, x) + C_{Bl}(t, x-h_x)] = r_{Bl} \quad \dots \quad 18$$

Solving eqn. (18) for $C_{Bl}(t+k, x)$, moving a head in time for C_{Bl} to obtain:

$$C_{Bl}^{(t+k, x)} = K_{Bl}^{t+K} \left[\frac{U_l}{h_x} + \frac{D_L}{h_x} \right] C_{Bl}^{(t, x+h_x)} - K_{Bl}^{t+K} \left[\frac{U_l}{h_x} + \frac{D_L}{h_x} \right] C_{Bl}^{(t, x)} + \frac{D_L K}{h_x} C_{Bl}^{(t, x-h_x)} \quad 19$$

To evaluate C_{Bl} in $(t+K)$ three values of C_{Bl} must be known. The evaluation is carried out by iteration procedure.

Before proceeding, we must solve a problem evolving from eqn. (19) at $X=0$;

$$\frac{\partial C_{Bl}(t, x)}{\partial X} \approx \frac{C_{Bl}(t, x+h_x) - C_{Bl}(t, x-h_x)}{2K} \quad 20$$

- At $X=0$

$$C_{Bl}(t, x-h_x) = C_{Bl}(t, h_x) - 2K \frac{\partial C_{Bl}(t, 0)}{\partial X} \quad 21$$

h_x is an increment of distance, while K is an increment of time. The values of X are limited to be lied between 0 and L inclusive while the values of t will increase indefinitely. Similarly equations (6, 7 and 9) are obtained in finite difference form for

$$C_{sI}(t+K, X), C_{O_2I}(t+K, X) \text{ and } C_{O_2g}(t+K, X)$$

7. Results and Discussion

7.1 Reliability of Model

To examine the reliability of the developed model, it was tested with experimental data excited in relevant literatures, [3, 21, and 22]. The experimental parameters are shown in table(1)

| Table (1): Experimental values in simulation (at 25° C) | | | |
|---|-----------------------|---------------------------------------|--|
| Parameter | Experimental Value | Units | Ref. |
| D_L | 1.5×10^{-5} | cm^3/s^2 | Abhishek Soni,[21] |
| D_c | 9.4 | cm | M.K. Gowthaman, N.P. Ghildyal, et. al ,[3] |
| K_{La} | 1.87×10 | cm/s | M.K. Gowthaman, N.P. Ghildyal, et. al ,[3] |
| H | 4.38×10^4 | (-) | M.K. Gowthaman, N.P. Ghildyal, et. al ,[3] |
| L | 75 | Cm | M.K. Gowthaman, N.P. Ghildyal, et. al ,[3] |
| r_B | 0.043 | $\text{g}/\text{cm}^3 \cdot \text{s}$ | M.K. Gowthaman, N.P. Ghildyal, et. al ,[3] |
| U_g | 1.06 | cm/s | M.K. Gowthaman, N.P. Ghildyal, et. al ,[3] |
| U_L | 0.5036 | cm/s | M.K. Gowthaman, N.P. Ghildyal, et. al ,[3] |
| ρ_{bd} | 0.03 | g/cm^3 | M.K. Gowthaman, N.P. Ghildyal, et. al ,[3] |
| ε_g | 0.5 | (-) | M.K. Gowthaman, N.P. Ghildyal, et. al ,[3] |
| K_o | 1.62×10^{-5} | s^{-1} | P. aarne Vesilind, J. Jeffery Peirce,[22] |

A comparison between experimental and simulated results for dissolved oxygen concentration in a (SBR) is shown in Figure (2). The figure shows a good agreement over the hole bed height.

It can be seen that oxygen concentration profile has a steep decrease at the lower part of the reactor while it almost has a constant value at the upper part of the reactor.

The reason for this behavior may be that the concentrations of reactants have much higher values in the lower part of reactor which leads to higher rates of reaction while in the upper part an equilibrium condition may existed between the reactants and products. The absolute average error between model and experimental results was 4.3%.

The developed model for the (SBR) can describe the hydrodynamic characteristics in addition to the oxygen consumption rate. The operation parameters such as the superficial velocities for gas and liquid influenced the performance of SBR since these parameters affect the bed porosity and expanded bed height. Figure (3.a, b) shows that the dissolved oxygen concentration and biomass concentration are slightly affected by the superficial gas velocity. It is seen that the oxygen transfer rate from the gas phase increased as superficial gas velocity increases because the mass transfer coefficient and the oxygen concentration in gas phase is

moderately related to the superficial gas velocity.

Biomass concentration seems to depend on solid holdup which is a function of superficial gas velocity, so biomass concentration increases slightly as the superficial gas velocity increased. Figure (4.a, b) shows the effect of superficial liquid velocity on dissolved oxygen concentration and biomass concentration in the liquid phase. It seems that these concentrations are highly affected by superficial liquid velocity in compared with the superficial gas velocity which is shown in figure (3) The contact time needed for microbes to utilize dissolved oxygen decreases when the superficial liquid velocity increased, so the rate of oxygen. The contact time needed for microbes to utilize dissolved oxygen decreases when the superficial

The contact time needed for microbes to utilize dissolved oxygen decreases when the superficial liquid velocity increased, so the rate of oxygen consumption decreased and consequently the existing dissolved oxygen concentration goes up. Biomass concentration is strongly affected by liquid superficial velocity because solid holdup is more affected by superficial liquid velocity.

Figure (5.a, b) shows the concentration profiles of the oxygen in the gas and the liquid phase. The oxygen profile for the gas phase decrease

continuously to 0 at the beginning of the process. While with the time due to the liquid phase saturation with oxygen and decreased driving force (i.e., the flux through the bubble interface), the profile flatters until the constant values along the end of the reactor. In the liquid phase, a maximum in dissolved oxygen concentration is observed. It is to notice that the curves are steeper and the phase saturation values are reached in short period. The possible explanation of this fact is the existence of supplementary diffusion resistance in the bubble.

8. Conclusions

The transient model which was formulated and validated to analyze the slurry bioreactor system in the bubbly flow regime led to the followings:

- The oxygen transfer rate from the gas phase increased slightly as the superficial gas

velocity increases because mass transfer coefficient and the oxygen concentration in gas phase are strongly related to superficial gas velocity.

- The dissolved oxygen concentration and biomass concentration are more affected by superficial liquid velocity than that by superficial gas velocity.
- For unsteady state, the oxygen concentration profile in gas and liquid follow a different behavior. In gas phase the concentration profile drops continuously to zero at the top of the reactor, while in liquid phase the concentration profile has a maxima and then it drops gradually to zero along the reactor, the latter behavior was repeated at each time increment

9. Nomenclatures

| Symbol | Definition | Unit |
|-----------|--|-------------|
| B_I | Biomass concentration | g/cm^3 |
| b | stoichiometric coefficient | (-) |
| C | Oxygen concentration | g/cm^3 |
| C_A | Concentration of O_2 at the outer surface of the microbial biomass layer | g/cm^3 |
| C_{BI} | Biomass concentration in the liquid phase | g/cm^3 |
| C_g | Concentration of O_2 in the gas phase | g/cm^3 |
| C_L | Oxygen concentration in the liquid phase | g/cm^3 |
| C_s | starch concentration | g/cm^{3p} |
| C_E | Concentration of the enzyme | g/cm^3 |
| C_{SL} | Concentration of the substrate in the liquid phase | g/cm^3 |
| D_g | effective diffusivity of O_2 in the gas phase | cm^2/s^2 |
| D_e | effective diffusivity of O_2 in the microbial biomass layer | cm^2/s^2 |
| D_E | effective diffusivity of the enzyme within the substrate | cm^2/s^2 |
| D_L | effective diffusivity of O_2 in the liquid phase | cm^2/s^2 |
| D_e | effective diffusivity of O_2 | cm^2/s^2 |
| e_b | molar density of the substrate | |
| g | Gravitational acceleration=9.81 | m/s^2 |
| H | Henry constant | (-) |
| h_x | increment of distance | Cm |
| K | Increment in biomass concentration | g/cm^3 |
| K_{cat} | catalytic constant of the enzyme | g/cm^3 |
| K_{LA} | Mass transfer coefficient | cm/s |
| K_{O_2} | saturation constant of oxygen | g/cm^3 |
| K_s | Michaelis-Menten constant for starch | (-) |
| K_0 | intrinsic zero-order rate constant | s^{-1} |
| L, l_c | overall particle size, length of the undegraded core of residual substrate | cm |
| M_{Ox} | | |
| r | radial position in the particle | cm |
| $r_{B,l}$ | Biomass consumption rate in liquid | g/cm^3sec |
| r_{O_2} | Oxygen consumption rate | g/cm^3sec |

| Symbols | Definitions | Units |
|-----------|--------------------------------|--------------------|
| t | Increment in time | s |
| U_g | Superficial gas velocity | m/s |
| U_L | Superficial liquid velocity | m/s |
| X | Biomass concentration | gm/cm ³ |
| Y_{O_2} | Yield of biomass upon oxygen | (-) |
| Y_s | Yield of substrate upon oxygen | (-) |
| Y_{O_x} | | |
| Z | | |

| Greek Symbols | Definition | Unit |
|---------------|-------------------------------|-------------------|
| ϵ_g | Gas hold-up | (-) |
| μ_m | Maximum specific growth rate. | s ⁻¹ |
| ρ_g | Density of gas | g/cm ³ |
| ρ_{ds} | Substrate dry density. | g/cm ³ |

10-References:

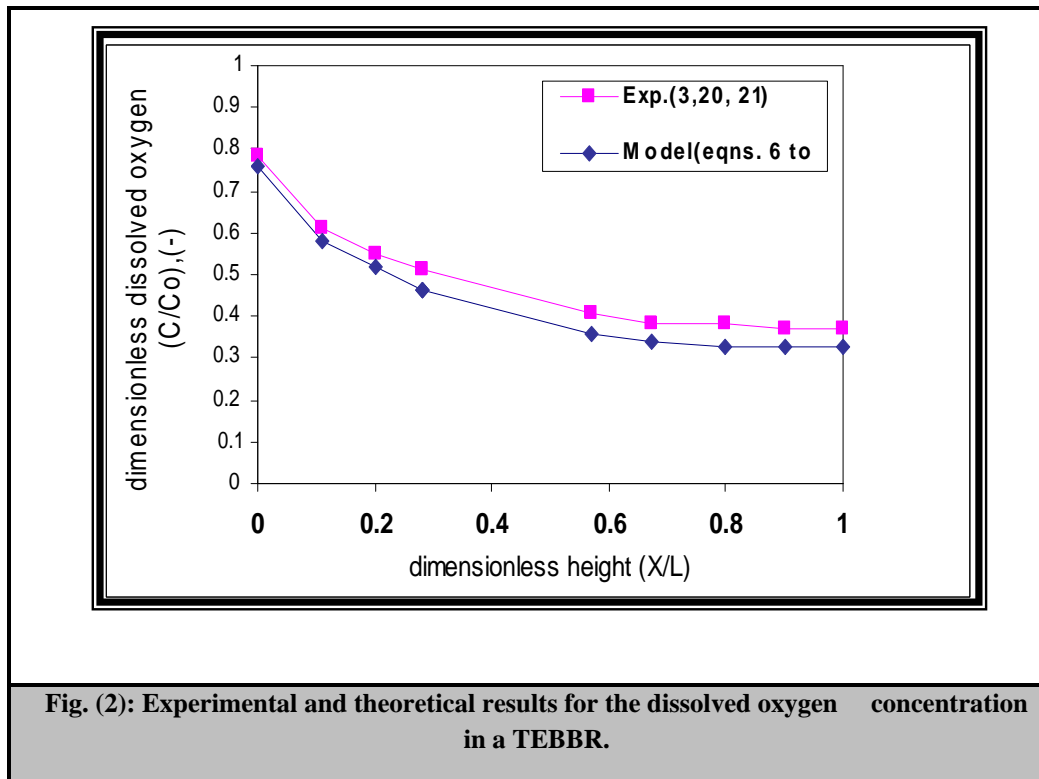
1. D.A. Mitchell, O.F. von Meien, N. Krieger, Recent developments in modeling of solid – state fermentation: Heat and mass transfer in bioreactors, *Biochem. Eng. J.* 13(2002) 137-147.
2. D.A. Mitchell, D.M. Stuart, R.D. Tanner, Solid-State fermentation microbial growth kinetics, in: M.C. Flickinger, S.W. Drow (Ed). *The Encyclopedia of Bioprocess Technology: Fermentation, Biocatalysis and Bioseparation*, vol. 5, Wiley, New York (1999),pp. 2407-2429.
3. M.K. Gowthaman, N.P. Ghildyal, K.S.M.S. Raghava Rao, N.G. Karanth, Interaction of transport resistances with biochemical reaction in packed bed solid-state fermenters: the effect of gaseous concentration gradients, *J. Chem. Technol. Biotechnol.* 56 (1993), 233-239.
4. N.P. Ghildyal, M.K. Gowthaman, K.S.M.S. Raghava Rao, N.G. Karanth, Interaction between transport resistant with biochemical reaction in packed bed solid-state fermenters: effect of temperature gradients, *Enzyme Microb. Technol.* 16(1994) 253-257.
5. S. Rajagopalan, J.M. Modak, Heat and mass transfer simulation studies for solid-state fermentation process, *Chem. Eng. Sci.* 49 (1994) 2187-2193.
6. P. Sangsurasak, D.A. Mitchell, Incorporation of death kinetics into a 2-D dynamic heat transfer model for solid-state fermentation, *J. Chem. Technol. Biotechnol.* 64 (1995) 253-260.
7. P. Sangsurasak, D.A. Mitchell, Validation of a model describing 2-dimentional heat transfer during solid-state fermentation in packed bed bioreactors, *Biotechnol. Bioeng.* 60(1998) 739-749.
8. D.A. Mitchell, A. Pandey, P. Sangsurasak, N. Krieger, Scale-up strategies for packed bed bioreactors for solid-state fermentation, *Process Biochem.* 35(1999) 167-178.
9. D.A. Mitchell, O.F. von Meien. Mathematical modeling as a tool to investigate the design and operation of the Zymotis packed-bed bioreactor for solid-state fermentation, *Biotechnol.* 68(2000) (127-135).
10. J. Sargantanis, M.N. Karim, V.G. Murphy, D. Ryoo, R.P. Tengerdy, Effect of operating conditions on solid substrate fermentation, *Biotechnol. Bioeng.* 42 (1993)149-158.
11. D.M. Stuart, Solid-State fermentation in rotating drum bioreactors, PhD. Thesis, The University of Queensland, Brisbane, Australia, (1996).
12. F.J. Weber, J. Tramper, A. Rinzema, A simplified material and energy balance approach for process development and scale-up of *Coniothyrium minitans* conidia production by solid-state cultivation in a packed-bed reactor, *Biotechnol. Bioeng.* 65(1999) 447-458.
13. G. Georgiou, M.L. Shuler, A computer model for the growth and differentiation of a fungal colony on solid substrate, *Biotechnol. Bioeng.* 28(1986) 405-416.
14. D.A. Mitchell, D.D. Do, P.F. Greenfield, H.W. Doelle, A semi-mechanistic mathematical model for growth of *Rhizopus oligosporus* in a model solid-state fermentation system, *Biotechnol. Bioeng.* 38(1991) 353-362.
15. S. Rajagopalan, J.M. Modak, Evaluation of relative growth limitation due to depletion of glucose and oxygen during fungal growth on a spherical solid particle, *Chem. Eng. Sci.* 50(1995)803-811 .
16. Octave Levenspiel, *Chemical Reaction Engineering*, 3rd edition, Joohn Wiley and Sons, (1999).
17. J. Oostra, E.P. le Comte, J.C. van den Heuvel, J. Tramper, A. Rinzema, Intra-particle oxygen diffusion limitation in solid-state fermentation, *Biotechnol Bioeng.* 74(2001) 13-24.
18. Y.S.P. Rahardjo, F.J. Weber, E.P. le Comte, J. Tramper, A. Rinzema, Contribution of

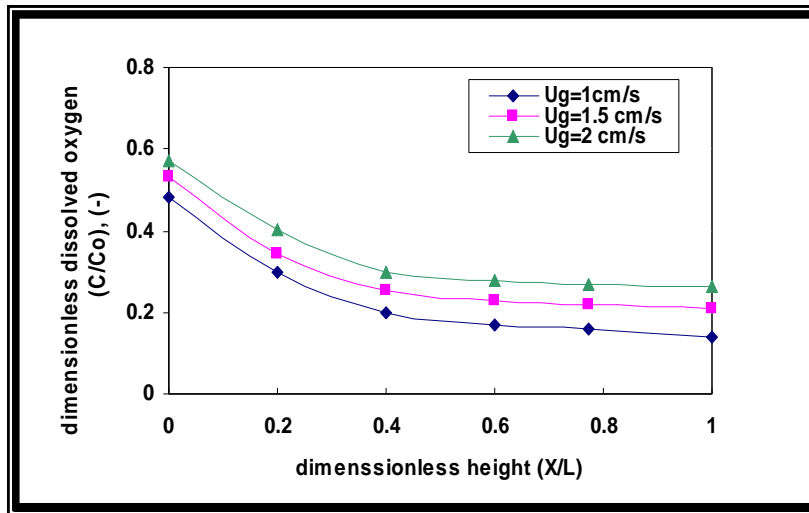
aerial hyphae of *Aspergillus oryzae* to respiration in a model solid-state fermentation system, *Biotechnol. Bioeng.*, in press, (2002).

19. S. Rajagopalan, D.A. Rockstraw, S.H. Munson-McGee, Modeling substrate particle degradation by *Bacillus coagulans* biofilm, *Bioresour. Technol.* 61(1997) 175–183.
20. M.P. Nandakumar, M.S. Thakur, K.S.M.S. Raghavarao, N.P. Ghildyal, Mechanism of solid particle degradation

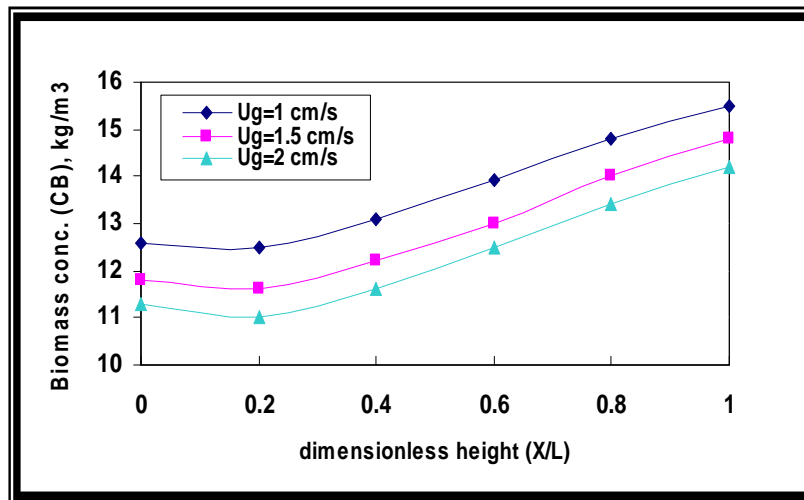
by *Aspergillus niger* in solid-state fermentation, *Proc. Biochem.* 29 (1994) 545–551.

21. Abhishek Soni (2002), A multi-Scale approach to fed-batch bioreactor control, M.sc thesis, University of Pittsburgh.
22. P. aarne Vesilind, J. Jeffery Peirce, Environmental Engineering, 1982



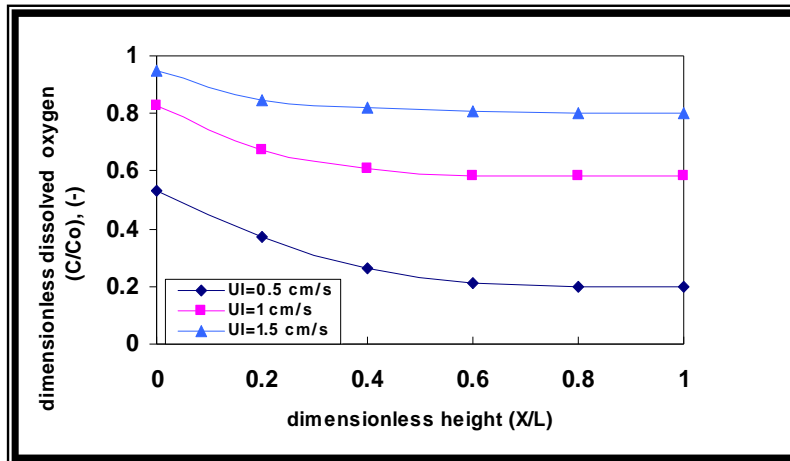


(a)

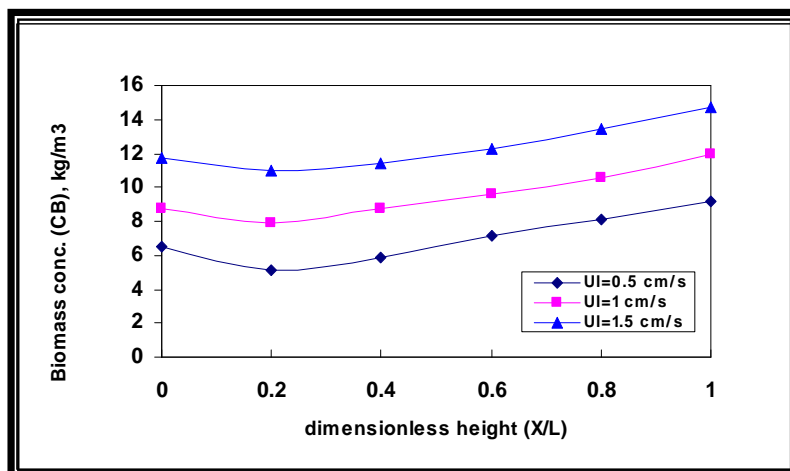


(b)

Fig. (3): Effect of superficial gas velocity on (a) the dissolved oxygen concentration and (b) biomass concentration at steady state.

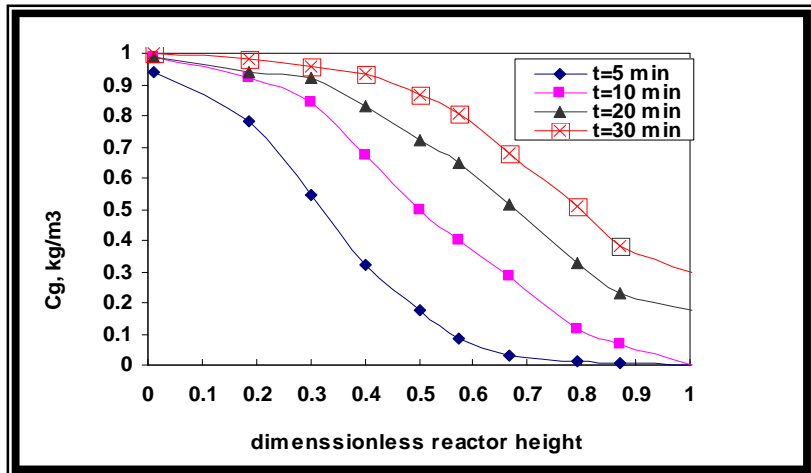


(a)

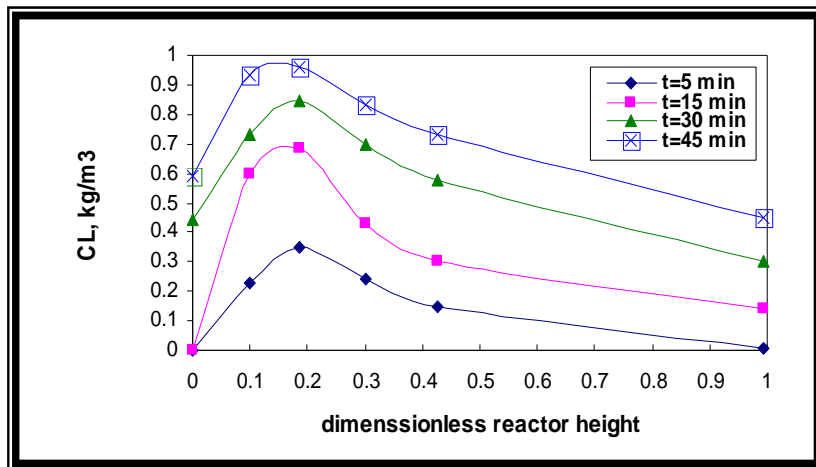


(b)

Fig. (4): Effect of superficial liquid velocity on (a) the dissolved oxygen concentration and (b) biomass concentration at steady state.



(a)



(b)

Fig.(5): Oxygen concentration profiles at different increments of time
(a) in gas phase (b) in liquid phase

"نمذجة توزيع الأوكسجين المذاب في المفاعل الأحيائي (البايولوجي) الثلاثي الطور"

م.م. سعد علاء الدين فائق
الجامعة التكنولوجية/قسم الهندسة
الكيميائية

م.م. أنيل خيري جابر
جامعة النهريين/ كلية الهندسة

أ.م.د. محمد فاضل عبد
الجامعة التكنولوجية/قسم الهندسة
الكيميائية

الخلاصة:

يهتم البحث بإيجاد موديل رياضي للتنبؤ بتراكيز الأوكسجين المذاب والمواد المتفاعلة الأخرى والمنتجة على الامتداد الطولي للمفاعل البايولوجي الثلاثي الطور الذي يعمل عند نظام الجريان المتجانس (Bubbly Flow Regime)

و يتكون الموديل من معادلات تفاضلية لتوازن الكتلة مع ادخال قانون معدل سرعة التفاعل لكل مادة من المواد المتفاعلة عند الحالة غير المستقرة (transient state).

ولتأكيد موثوقية الموديل تحت مقارنة نتائج الموديل مع نتائج عملية عند نفس الظروف التشغيلية و اعطت المقارنة معدل انحراف لايزيد عن % ٣.٤.

واوضح الموديل كيفية تأثير الظروف التشغيلية (سرعة الغاز والسائل) على تركيز المواد المتفاعلة و المنتجة على امتداد المفاعل حيث ان سرعة السائل لها تأثير اكبر من سرعة الغاز على معدل تغير التراكيز.

كما استخدم الموديل لبيان تغير التراكيز عند الحالة غير المستقرة.

الكلمات الدالة:- نمذجة، المفاعل البايولوجي، المفاعل الثلاثي الطور، معدل النمو.

This document was created with Win2PDF available at <http://www.daneprairie.com>.
The unregistered version of Win2PDF is for evaluation or non-commercial use only.